Numerical Analysis of Impact Induced Failure for MEMS Membranes during Guided Free Fall Tests

David Faraci[1], Aldo Ghisi[1], Silvia Adorno[2], Alberto Corigliano[1]
[1] Department of Civil and Environmental Engineering, Politecnico di Milano, piazza Leonardo da Vinci 32, 20133, Milano, Italy
[2] ST Microelectronics, via Tolomeo 1, Cornaredo (MI), Italy

Abstract

Impact effects on thin silicon MEMS membranes attached to dummy devices, as observed through guided free fall tests, are investigated through three-dimensional, finite element numerical simulations. Accounting for the different scales involved, a multiscale top-down approach is followed: fluid dynamics and solid mechanics macro-scale simulations are first carried out, to provide input histories for fluid (air) pressures and relative displacements for the thin silicon membrane anchors at the micro-scale. Then, a mechanical analysis is carried out for each membrane to judge whether possible failures arise in a given guided free fall test. It is found that in some cases possible failures actually depend from the combination of the fluid-induced and of the solid-induced input transferred to the MEMS membrane, and not from a single domain-induced loading condition.

1. Introduction

Many MEMS structures, attached to (macroscale) devices, e.g. mobile phones, subject to accidental drops have to sustain severe loadings [1-4]. In the case of MEMS microphones [5-6], thin silicon membranes under working conditions have to remain into communication with the outside air through narrow ducts, where the fluid can flow freely. Unfortunately, through the same passages sudden fluid pressure rises, such as the ones generated during the impact with a target surface (i.e. the floor), are also transferred to the thin membranes, making them prone to fail to this extreme (and not easily-estimated) loading condition.

The effect of impact against hard surfaces on these thin silicon MEMS membranes can be inspected through guided free fall (GFF) tests [7], in which the MEMS are set on an exemplary device, such as a dummy smartphone, also known as jig, that is driven downwards and then left to fall and collide against a rigid floor. Because the transmission of the impact stress waves inside the solid domain combines with a pressure rise in the fluid (air) surrounding the membrane, and since strongly varying loading conditions during the contact and the following bounce are present, an eventual failure of the thin structure becomes hard to predict and an accurate study is required. In absence of local information at MEMS level, at present it is possible to ascertain only a yes/no answer about the working condition of each sample and therefore there is a lack of any cause-effect relationship and any predictive ability on new design choices. In this work, three dimensional finite element simulations investigate local effects in terms of stress values and deformed configurations at the membrane (micro-scale) level, starting from macro-scale simulations of the falling jig in a GFF test.

2. Methodology

As mentioned above, the consequences of the MEMS design on the impact resistance are typically industrially evaluated by means of an experimental setup replicating an accidental drop of a commercial (portable) device in which the MEMS component finds its application. In our case, an apparatus with a rack nut (Figure 1a) drags down and then releases (at a specified height of half a meter) a dummy smartphone specimen (a.k.a. jig), consisting in an aluminum base and a steel core, see Figure 1b. Since the first part of the fall occurs along the vertical direction with the jig attached to the machine, the test is called a "guided" free fall.

(a)

(b)

Figure 1: (a) detail of the specimen fixing to the drop machine; (b) exemplary jig (before the addition of the MEMS devices).

A high-speed camera (see e.g. [8]) tracks the last part of the fall till the specimen impacts the hard granite ground. After each fall, it is possible to inspect the working condition of each MEMS device, obtaining a working/not working result. Unfortunately, at present this is the only information available during the tests, hence a numerical simulation approach is necessary to enlighten the possible causes for each failure or malfunctioning.

In this work, the displacement histories of the falling jig, captured by a high-speed camera, are applied as input for a macro-scale fluid-structure interaction analysis. In the latter, the air surrounding the jig is also modelled and the jig surfaces are treated as movable walls, displacing in accordance to the aforementioned experimental measurements. The solid domain (jig) and the fluid domain (air) interact through the mentioned movable jig surfaces.

Figure 2 shows a typical model for the fluid-structure interaction macro-scale analysis. The jig (with a simplified geometry) is placed at a small distance from the ground impact surface, on the order of 20 or 40 mm, therefore neglecting the influence of the pressure rise during the fall except for the last instants. Since the object has been inspected during the fall through the high-speed camera, the initial configuration at the set distance from the target impact surface can be carefully modelled, i.e. accounting for the two inclination angles around the jig axes. Moreover, the initial speed, as experimentally observed, is applied to the exterior walls of the jig. The motion of the jig during the fall is modelled through the known displacement functions applied to the movable walls of the fluid domain, coincident with the jig exterior surfaces; the fluid dynamics domain is also subject to (possible) re-meshing at stated time intervals, whenever the fluid elements become too distorted. In particular, in the neighboring of the impact event the fluid gap becomes very small, and the analysis time step is correspondingly reduced; the re-meshing procedure therefore becomes necessary and quite demanding. Several algorithm parameters actually affect the success of the analysis, in particular the initial and current mesh size during the impact, the time step for the transient solution, the accepted distortion for the finite elements. However, despite the pressure rise during the last instants before the impact, the fluid velocity remains value-limited, so that a laminar fluid hypothesis has been considered. Other boundary and initial conditions are set as follows: i) the initial condition for air is at atmospheric pressure, ii) all the wall fluid surfaces are in/out walls at atmospheric pressure, iii) except for the ground impact surface, which is a non-movable wall excluding any flux orthogonal to it, iv) finally, the jig surfaces are also treated as zero-flux walls except for the four small entrance surfaces (Figure 2b) leading into the small volume where each MEMS is placed. The whole fluid-structure model includes about 90,000 nodes and 460,000 tetrahedral elements.

Consequently, we can calculate the pressure histories at the inlet of the narrow ducts (placed on the jig bottom surface, see the arrows in Figure 2a and Figure 2b) leading into the chamber where the MEMS membranes are placed. Because of the difference in the scales involved, ranging from ten centimetres for the jig down to the one-micrometre membrane thickness, a multiscale top-down approach is needed: the macro-scale fluid pressure history during the impact is transferred as input at the meso-scale, see Figure 2b, where only the fluid inside the duct is modelled, and finally at the micro-scale, where only the silicon membrane is modelled, see Figure 2c.

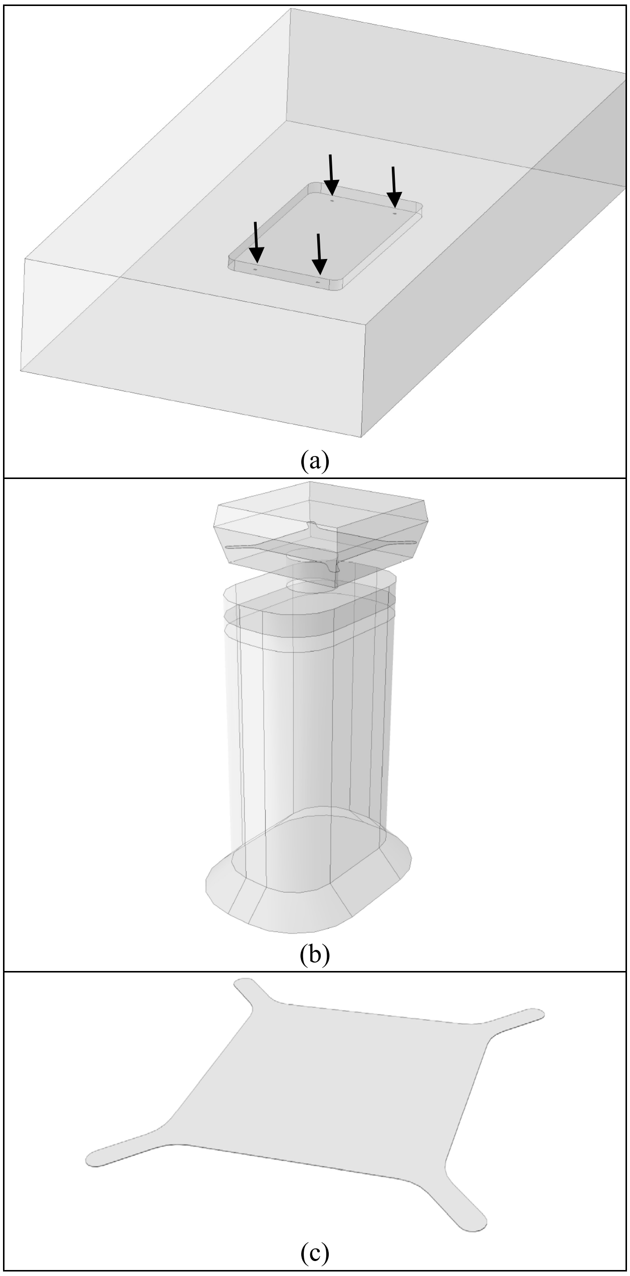

Figure 2: (a) macro-scale model including jig and surrounding air, arrows indicate (b) the narrow ducts whose air domain is described at the meso-scale model; (c) micro-scale model made of a thin silicon membrane.

A second macro-scale analysis (with about 650,000 nodes and 400,000 elements) is also carried out, accounting for a purely mechanical domain for the jig impacting against the ground (i.e. neglecting air): the macro-scale displacement time-histories of the membrane anchor points are registered and, similarly to the fluid-dynamic case, they are then transferred as input to the micro-scale 1µm-thick membrane model. The latter model (accounting for only 6,000 nodes and as many shell elements), with the aforementioned fluid pressure and displacement transient histories as input, is then analysed through an implicit dynamics, mechanical analysis, allowing for large displacements and contact with neighboring surfaces, and the status of the membrane is checked for possible failures.

3. Results

Repetition of the GFF tests shows that eventual membrane failures are hardly predictable from nominally equal initial conditions, but unavoidable imperfections strongly influence the way the jig impacts and rebounds against the granite floor. Henceforth, local information of the impact history helps to clarify the failure behavior and possibly its causes, provided the accurate numerical analyses described above are carried out.

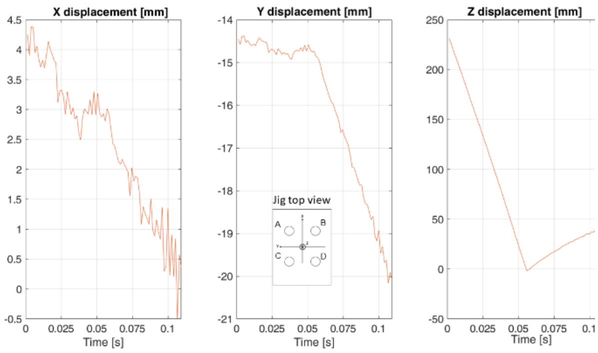

(a)

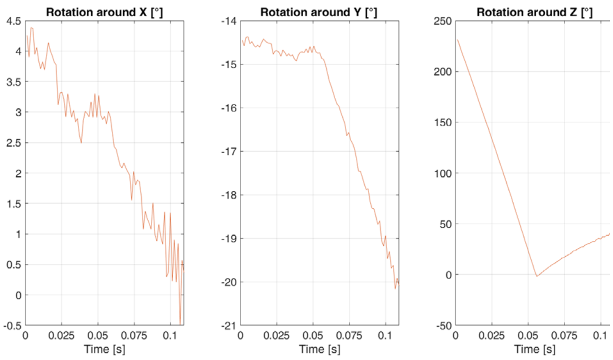

(b)

Figure 3: (a) experimental displacements at the origin of the reference system on the jig top surface during the guided free fall test; (b) corresponding rotations around the axes.

In Figure 3 an exemplary history of displacements and rotations for the jig top surface reference point used for the high-speed camera observations are shown. Only the information for the last 20 mm of falling distance has been used in the next results; moreover, the attention is focused mostly to the first impact, while further contacts with the ground are reasonably occurring at lower energy (i.e. velocity). Therefore, only 10 ms of the whole time history observed through the high-speed camera is actually considered, around the first impact time. During the fluid-structure analysis the pressure is oscillating in time (see Figure 4), with an amplitude which is obviously increasing when the jig approaches the impact surface, then a depression phase follows with more pressure oscillations. In Figure 5 streamlines of the velocity show the fluid spillage below the jig during the impact and the air recirculating and generating the oscillating pressure on the lower jig surface.

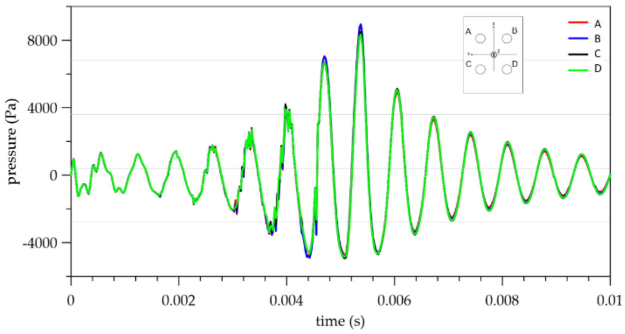

Figure 4: pressure histories at the entrance of the four ducts leading to the silicon membrane chamber.

By looking at the (over)pressure histories at the four duct entrances, shown in Figure 4, it appears that there is not a clear difference between the four sensors at the jig vertices. However, the experimental evidence shows that often only one of the sensors has a “failure”, while the other three remain “undamaged”, provided that a breaking here is simply a MEMS not working anymore, for whatever reason.

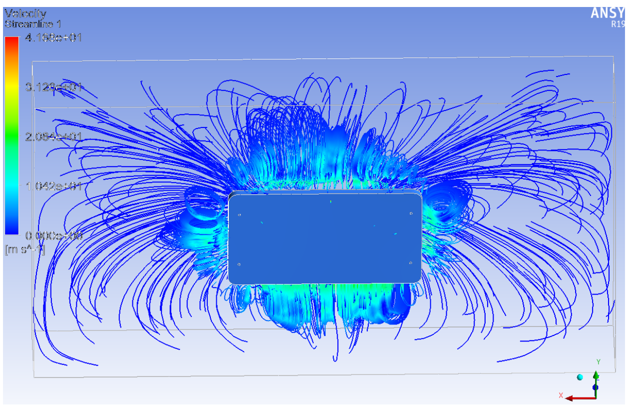

Figure 5: streamlines of the velocities during the impact between the jig and the ground surface.

It is not reported here for brevity, but the meso-scale fluid-dynamic analysis (Figure 2b), considering the air duct leading to the membrane, aand based on the application at the inlet of the meso-scale pressure, does not show a significant pressure variation between the inlet and the reservoir around the silicon membrane.

Hence, a conjecture has been proposed: in some cases, the failure is not only pressure-induced (i.e. caused by air pressure rise/decrease) or only solid-induced (i.e. caused by the stress waves propagating in the jig and reaching the membranes through their anchors), but it is the combination of the two phenomena to matter.

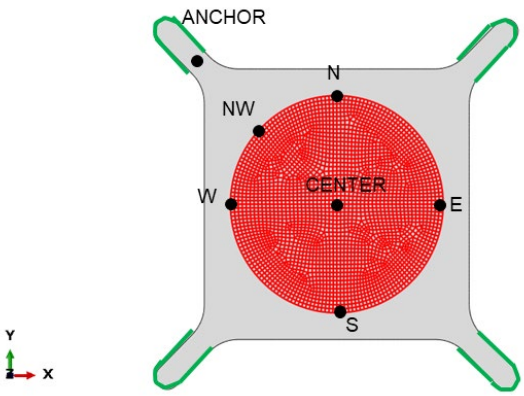

Figure 6: loading conditions for the micro-scale analysis on the silicon membrane. The surface, on which the pressure history (obtained from the macro-scale fluid dynamics analysis) is applied, is represented in red color, while the relative displacements (due to the stress waves travelling in the solid) are imposed along the green boundaries.

To check this idea, in addition to the pressure history assigned to a central surface on the membrane (see Figure 6), the displacement histories of the four anchors where each membrane is attached to its substrate, have been also included at the micro-scale level. It is worthwhile to recall that the input displacements have been considered in a local reference system joint with a substrate plane to which three anchor points belong. Moreover, there is a time delay between the air pressure increase due to the approaching ground impact surface and the effect of the stress waves travelling in the jig solid parts to the membrane anchors: in the analyses this time delay has been deterministically accounted for.

Figures 7 and 8 report the stresses at the points shown in Figure 6 at the lower surface of the membrane. The stresses appear low at the center of the membrane, while they increase significantly at the anchors when the relative displacements are included. It also worth to mention that in Figure 7 the time envelopes of the maximum principal stress for all the points of a region near the anchor is represented. However, in correspondence of the appearance of the anchor motions, the (over)pressure reaches its maximum amplitude in the oscillations, and therefore the two phenomena combine in a complex way.

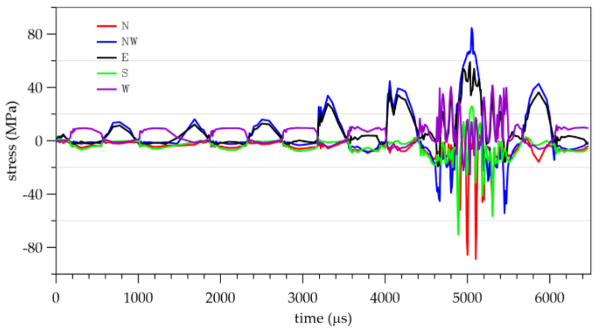

Figure 7: maximum principal stresses at the membrane points depicted in Figure 6 during the first impact.

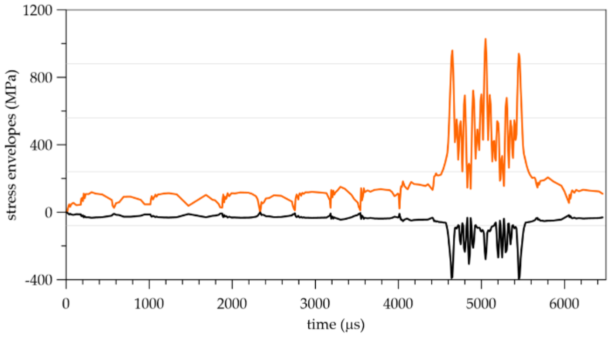

Figure 8: envelopes of principal stresses at the membrane anchor region depicted in Figure 6 during the first impact.

While the membrane oscillation shape is predictable if only the (over)pressure is applied, the combination of stretching and buckling due to the in-plane imposed relative displacements is responsible of a complex pattern of deformed configurations, some of which are represented in Figure 9.

4. Conclusions

To identify the causes of mechanical failure in thin silicon membranes used in MEMS microphones, numerical simulations replicating guided free fall tests have been carried out. Both fluid dynamics and mechanical analyses seem necessary to correctly apply the input necessary for the evaluation of the membrane status during the impact with the ground, since in some cases the failure does not depend only from the air pressure increase/decrease or only from the travelling stress waves inside the solid, but from the combination of the two phenomena.

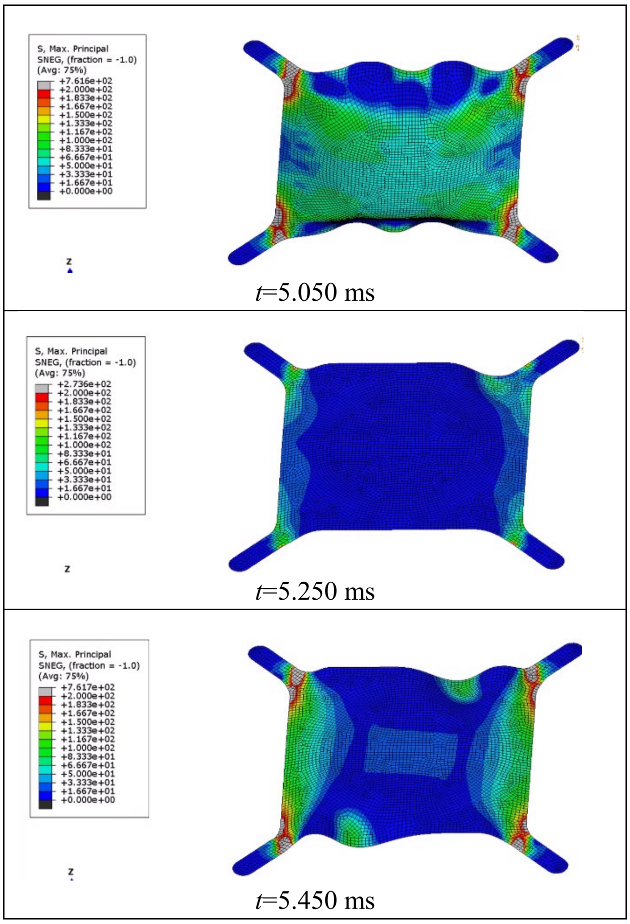

Figure 9: exemplary patterns of the deformed membrane configuration during the application of the relative anchor motions and air pressure. Displacement magnification set to 10.

Acknowledgments

We thank Emanuele Zappa for the high-speed camera observations and Mattia Vandi for the help during the guided free fall tests.

References

1. Mariani, S, Ghisi, A, Corigliano, A, Zerbini, S, "Multi-scale Analysis of MEMS Sensors Subject to Drop Impacts," *Sensors*, Vol. 7 (2007), pp. 1817-1833.
2. Mariani, S, Ghisi, A, Fachin, F, Cacchione, F, Corigliano, A, Zerbini, S, "Multiscale analysis of polysilicon MEMS sensors subject to accidental drops: effect of packaging," *Microelectronics Reliability*, Vol. 49 (2009), pp. 340–349.
3. Mariani, S, Martini, R, Ghisi, A, Corigliano, A, Beghi, M. Two-scale simulation of drop-induced failure of polysilicon MEMS sensors," *Sensors*, Vol. 11 (2011), pp. 4972-4989.
4. Corigliano, A, Ardito, R, Comi, C, Frangi, A, Ghisi, A, Mariani, S, Mechanics of Microsystems, John Wiley & Sons Ltd (2018), Chapter 13.
5. J. Meng, J, Douglas, S T, and Dasgupta, A, "MEMS Packaging Reliability in Board-Level Drop Tests Under Severe Shock and Impact Loading Conditions–Part I: Experiment," *IEEE Transactions on Components, Packaging and Manufacturing Technology*, Vol. 6 (2016), pp. 1595-1603.
6. Nicollini, G, Devecchi, D, "MEMS Capacitive Microphones: Acoustical, Electrical, and Hidden Thermal-Related Issues," *IEEE Sensors Journal*, Vol. 18 (2018), pp. 5386-5394.
7. Tempelman, E, Dwaikat, MMS, Spitás, C, "Experimental and Analytical Study of Free-Fall Drop Impact Testing of Portable Products", *Experimental Mechanics,* Vol. 52 (2012), pp. 1385–1395.
8. Lall, P, Panchagade, D, Iyengar, D, Shantaram, S, Suhling, J, Schrier, H, "High Speed Digital Image Correlation for Transient-Shock Reliability of Electronics," *Proceedings 57th Electronic Components and Technology Conference*, Reno, NV, 2007, pp. 924-939.